

An Enhanced UNB Ionospheric Modeling Technique for SBAS: The Quadratic Approach

Hyunho Rho and Richard B. Langley

Department of Geodesy and Geomatics Engineering, University of New Brunswick, Fredericton, N.B. Canada

Attila Komjathy

NASA Jet Propulsion Laboratory / California Institute of Technology, Pasadena, CA, USA

BIOGRAPHY

Hyunho Rho received an M.Sc. in 1999 in geomatics from Inha University, South Korea. He is currently a Ph.D. candidate in the Department of Geodesy and Geomatics Engineering at the University of New Brunswick (UNB), where he is investigating ways to improve ionospheric modeling for wide area differential GPS (DGPS).

Richard Langley is a professor in the Department of Geodesy and Geomatics Engineering at UNB, where he has been teaching since 1981. He has a B.Sc. in applied physics from the University of Waterloo and a Ph.D. in experimental space science from York University, Toronto. Prof. Langley has been active in the development of GPS error models since the early 1980s and is a contributing editor and columnist for GPS World magazine. He is a fellow of the ION and shared the ION 2003 Burka Award.

Attila Komjathy is currently a staff member of the Ionospheric and Atmospheric Remote Sensing (IARS) group specializing in remote sensing techniques using the Global Positioning System. Prior to his joining JPL in July 2001, he worked on the utilization of GPS reflected signals as a research associate at the University of Colorado's Center for Astrodynamics Research. He received his Ph.D. from UNB's Department of Geodesy and Geomatics Engineering in 1997. He is a member of the WAAS Integrity and Performance Panel (WIPP).

ABSTRACT

Several satellite-based augmentation systems (e.g., WAAS, EGNOS, and CDGPS) have recently started operations and more are planned for the future. With a view towards further improving the accuracy of such systems, the associated ionospheric modeling technique is capturing the attention of the scientific community. As long as the ionosphere is the biggest error source in single-frequency GPS, the accuracy of ionospheric modeling remains a critical issue in satellite-based

augmentation systems. In terms of modeling the ionosphere, the current UNB approach uses a bi-linear approximation and so ignores the non-linear spatial variation of the ionosphere over the monitoring stations. Efficiency and an acceptable level of accuracy are the main reasons for using a simplified linear model. However, we are left with the questions: Is the linear model sufficient to explain the temporal and spatial variations of the ionosphere? What are the effects of ignoring the non-linear spatial variations in the ionosphere especially under geomagnetic storm conditions?

To provide answers to these questions, we have extended the UNB ionospheric modeling technique from bi-linear to the quadratic form. As the quadratic model is far more sensitive to the distribution of the ionospheric pierce points (IPPs) than the linear model, there are a number of risks in adopting this potentially higher fidelity model. The main risk is associated with the uneven distribution of data and even data holes (although this can be overcome by a threat model which looks at the undersampled and temporal threats) which can lead to spurious spikes and unphysical features in the resulting models.

To test our new model, we have mainly used data from the U.S. Continuously Operating Reference Stations (CORS) network and the International GPS Service (IGS) network. With this relatively dense combined network, we have minimized data gaps. A data set spanning one month from October 25 to November 25, 2003 has been used to generate statistics. On October 29, 30, 31 and November 20, 21, 2003, there were significant geomagnetic disturbances.

We first examined the effect of "not-monitored satellites" on the estimator. In a global ionospheric model, all the satellites are monitored by a global scale network (all satellites are seen by at least one station at all times). However in a regional ionospheric model, only some of satellites can be seen by the ground network at the given

time. We quantified the differences between the global approach and regional approach. On a quiet day, the difference in rms of residuals was about 0.25 TECU and it was 0.5 TECU when the ionosphere was disturbed.

We also examined the quantified differences between the two approaches, the quadratic and bi-linear models, using data sets from both quiet days and days when the ionosphere was disturbed. In quiet conditions, the improvements of daily rms of residuals are at about the 1 (maximum 1.5 TECU) TECU level or less. The maximum improvement in rms of residuals happens when the ionosphere is significantly disturbed. The level of improvements is at the 1 to 3 TECU level. We also discuss the advantages and disadvantages of the two approaches that we encountered during the research.

For validation purposes and to see if there exist any unphysical or abnormal features in our models, we compared the estimated ionospheric vertical delays from both the bi-linear and quadratic models with those of WAAS. With the quadratic model, there was a better agreement with WAAS at the level of 23cm. However overall peak-to-peak variations of estimated VTECs from both UNB quadratic and bi-linear models are within the uncertainties (one sigma) of WAAS.

The presented results could serve as a baseline for further improvements in the GPS-based ionospheric modeling techniques for satellite-based augmentation systems.

INTRODUCTION

In recent years, several satellite-based augmentation systems (e.g., WAAS, EGNOS, and CDGPS) have started operations and more are planned for the future. As long as the ionosphere is the biggest error source in single-frequency GPS, the accuracy of ionospheric modeling remains a critical issue in satellite-based augmentation systems.

A number of ionospheric modeling techniques have been investigated and suggested for wide area DGPS (WADGPS) systems [El-Arini et al., 1994]. In terms of modeling the ionosphere, many authors have proposed use of polynomial expansions, grid-based techniques and spherical harmonics in latitude and longitude [Komjathy, 1997; Skone, 1998; Schaer, 1999]. In those two dimensional approaches, the vertical variation of the ionospheric electron density is absorbed into a thin shell at a pre-defined fixed height, approximately 350-450km. Further approaches have been proposed to account for the vertical variations in ionosphere [Juan et al., 1997; Mannucci et al., 1999; Komjathy et al., 2002]. Those models allow estimating the vertical variations in addition to the horizontal variation in the ionosphere by including two or more shells in the models. As an alternative

approach, Hansen [2002] proposed to use tomography for providing WADGPS ionospheric corrections by integration of densities in the vertical dimension.

Those three-dimensional models can more precisely estimate the model parameters when the ionosphere is undergoing high spatial and temporal variations, such as during disturbed ionospheric conditions. However as more coefficients need to be estimated, more data and more processing time are needed.

The current UNB approach for ionospheric modeling use a two-dimensional spatial linear model for the basis functions. Efficiency and an acceptable level of accuracy are the main reasons for using the simplified linear model. However, we are left with two questions unanswered: Is the linear model sufficient to explain the temporal and spatial variations of the ionosphere? What are the effects of non-linear spatial variations in the ionosphere especially under geomagnetic storm conditions?

To provide answers to these questions, we have extended the UNB ionospheric modeling technique from bi-linear to the quadratic form. A few authors have already used a quadratic approach to model the ionosphere. Coco et al. [1991] used a quadratic model to estimate the satellite inter-frequency biases (IFB). Wielgosz et al. [2003] recently used a multi-quadratic approach for regional ionospheric modeling. In our approach, since the quadratic model is far more sensitive to the density and distribution of the ionospheric pierce points (IPPs) than the linear model, we carefully selected 48 reference stations for the ionosphere modeling. We used stations mainly from the U.S. Continuously Operation Reference Stations (CORS) network and the International GPS Service (IGS) network.

In this paper, we first examine the “not-monitored” satellite effects for the regional ionospheric model. We also present the quantified differences between the two approaches, the quadratic and bi-linear models, using data sets from both quiet days and days when the ionosphere is disturbed. We also discuss the advantages and disadvantages of the two approaches that we encountered during the research. For validation purposes, we compared the vertical TEC, which can be retrieved from both bi-linear and quadratic models, with WAAS-derived values at each reference station.

UNB ESTIMATION STRATEGY

To generate ionospheric observables, the phase-levelling technique is used. The integer-ambiguity afflicted differences of the L1 and L2 (L1-L2) carrier phase measurements are adjusted by a constant value determined for each phase-connected arc of data using precise pseudorange measurements [Komjathy and

Langley., 1996]. The generated ionospheric observables are used to estimate the ionospheric vertical delays at each reference station by use of both the bi-linear and quadratic model. The elevation cut-off angle, 15 degrees, is used for the GPS measurements to minimize the elevation-angle dependent noise errors.

1) Bi-linear Model

$$TEC_r^s(t_k) = M(e_r^s) \cdot [a_{0,r}(t_k) + a_{1,r}(t_k) \cdot d\lambda_r^s + a_{2,r}(t_k) \cdot d\varphi_r^s] + b_r + b^s \quad (\text{eqn. 1})$$

where

$TEC_r^s(t_k)$ is the L1-L2 phase-levelled ionospheric observable at epoch t_k made by receiver r_j observing satellite s_i ,

$M(e_r^s)$ is the thin-shell elevation-angle mapping function projecting the vertical measurement (VTEC) to the line-of-sight measurement with elevation angle, e_r^s ,

$a_{0,r}, a_{1,r}, a_{2,r}$ are the parameters for spatial linear approximation of TEC to be estimated with an assumption of a first-order Gauss-Markov stochastic process,

$d\lambda_r^s = \lambda_r^s - \lambda_0$ is the difference between the longitude of an ionospheric pierce point and the longitude of the mean sun,

$d\varphi_r^s = \varphi_r^s - \varphi_r$ is the difference between the geomagnetic latitude of the ionospheric pierce point and the geomagnetic latitude of the station, and

b_r, b^s refer to the receiver and satellite differential delays (inter-frequency biases) respectively.

2) Quadratic Model

$$TEC_r^s(t_k) = M(e_r^s) \cdot [a_{0,r}(t_k) + a_{1,r}(t_k) \cdot d\lambda_r^s + a_{2,r}(t_k) \cdot d\varphi_r^s + a_{3,r}(t_k) \cdot (d\lambda_r^s)^2 + a_{4,r}(t_k) \cdot (d\varphi_r^s)^2 + a_{5,r}(t_k) \cdot (d\varphi_r^s \cdot d\lambda_r^s)] + b_r + b^s \quad (\text{eqn. 2})$$

where

$a_{3,r}, a_{4,r}, a_{5,r}$ are the second order surface parameters,

$(d\lambda_r^s)^2$ is the second order difference between the longitude of a ionospheric pierce point and the longitude of the mean sun,

$(d\varphi_r^s)^2$ is the second order difference between the geomagnetic latitude of the ionospheric pierce point and the geomagnetic latitude of the station.

The general Kalman filter approach was used to estimate the first and second order surface parameters in the models under the solar-geomagnetic reference system. As the dominant variation in the ionosphere is diurnal by nature, using a sun-fixed reference system, instead of an

Earth-fixed one, results in a more stable view of the ionosphere, and consequently more precise modeling.

Due to the highly varying ionospheric conditions on geomagnetically disturbed days during the one-month data set (see Figure 2), we used two different uncertainties for the dynamic model. For the ionospheric quiet condition days, we allowed the model to follow 1 TECU per 15 minute change in the total electron content, which resulted in the process noise variance rate of change being 0.001 TECU²/second characterizing the uncertainties of the dynamic ionospheric model. For storm condition days, we used a 0.008 TECU²/second value as the dynamic model uncertainty. This allowed the model to follow a relatively high 1 TECU per 2 minute change in the total electron content. For the variance of the measurement noise, we used 1 TECU² which describes the uncertainty in the observations. For the correlation time of states, we used 5 minutes corresponding to the WAAS update interval for ionospheric grid points.

Since we don't have a priori information about the absolute receiver and satellite IFBs, we fixed one receiver to estimate other IFBs with respect to this reference receiver. The Albert Head (ALBH) station (see the following Figure 1) was selected as the reference station. The ALBH station has relatively small measurement noise and consistently no data gaps for the whole period of one month. Although the satellite and receiver biases are time dependent, we assumed they are constant over a day. Sardon and Zarraoa [1997] showed the variation of satellite and receiver inter-frequency biases are small, typically less than 0.5ns for satellite biases and 1ns for receivers between consecutive days, as long as there is no hardware change. We used estimated satellite and receiver IFBs of the previous day, as a priori values for the daily process in a continuous one-month process.

The actual optimum ionospheric shell height is varying and there is a possible error in using a fixed shell height of 0.5 TECU for every 50km in the shell height [Komjathy, 1997]. However, to have more consistent comparisons with WAAS, we assumed the ionospheric vertical density has a median value at a fixed height, 350km, above the Earth's surface. An ionospheric shell height of 350km is the current assumption for WAAS.

DATA SETS

A total of 48 GPS reference stations from 8 different networks were used for the performance analysis. Dual-frequency GPS data from 24 Continuously Operating Reference Stations (CORS), 11 stations from the International GPS Service (IGS) reference network, 7 stations from the Forecast System Laboratory (FSL) array, 3 stations from the Bay Area Regional Deformation (BARD) network, one station from the Eastern Basin

Range Yellowstone (EBRY) array, a station from Southern California Integrated GPS Network (SCIGN) and the last station from the Western Canada Deformation Array (WCDA) have been used together to estimate ionospheric vertical delays at the stations by use of both the bi-linear and quadratic approaches. The 48 reference stations are located from latitude 24.5 degrees north to 50.9 degrees north and longitude 63.6 degrees west to 124.4 degrees west (see Figure 1). When data is not available from a station, a nearby station is used instead. Data from station AOML, Atlantic Oceanographic & Met Lab, was not available for Oct. 25-27 and just 1 to 4 % of daily data was available for Nov 11 and 12. We replaced this station by MIA3, Miami 3, for those five days.

For the purposes of comparison with WAAS ionospheric grid delays, we first selected a set of stations as close as possible to the WAAS Reference Stations (WRSs). As long as the density and distribution of data are also to be considered, we chose more stations to have more evenly distributed ionospheric measurements and to make sure there are no data holes in the area of coverage. A data set spanning one month from October 25 (DOY 298) to November 25 (DOY 329), 2003 has been used to generate statistics for the differences in estimated TEC between the bi-linear and quadratic approaches.

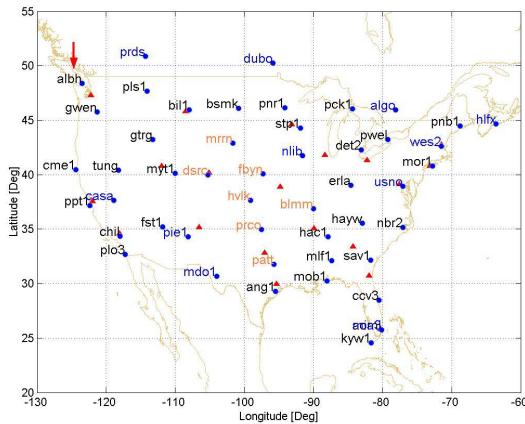


Figure 1. Forty-eight reference stations. The triangles with red color show the current 20 WAAS reference stations (WRSs) within the Conterminous United States and the blue circles show the 48 selected reference stations to model the ionosphere. The red arrow shows the reference station, which we used for satellite and receiver IFBs estimation. The station names with blue colors represent the monitoring stations from IGS, orange color shows the monitoring stations from FSL. The station PPT1, CASA and TUNG are from BARD array, the GTRG station from EBRY array and the CHIL station is from SCIGN array and finally the ALBH station is from WCDA. The other 24 stations are from the CORS network.

In order to accurately evaluate the effects of the quadratic approach, the duration of enhanced ionospheric activity must be identified. Two standard indices are used. Large negative Disturbance Storm Time (Dst) index values indicate the occurrence of a geomagnetic storm. The more negative the values are, the more intense the geomagnetic storm. The Kp index is used to confirm the geomagnetic storm time and magnitude. Figure 2 shows the Dst and Kp geomagnetic indices during the period of this research.

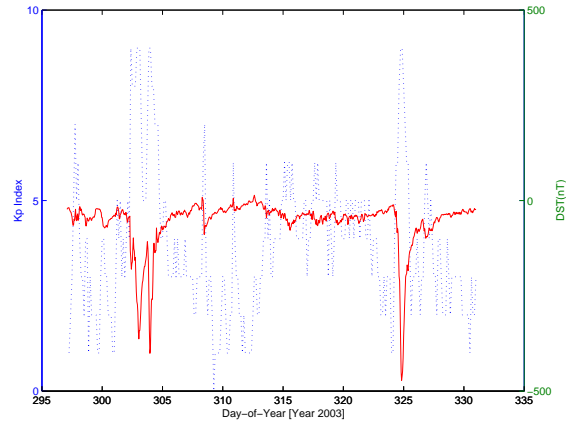


Figure 2. Dst and Kp indices from October 24 (DOY 297) to November 27 (DOY 331), 2003. The solid line (red) shows the Dst index and the dashed line (blue) shows the 3-hour Kp index.

For detailed views and analysis, we selected two sample days. On November 20, 2003 (DOY 324), there was a significant geomagnetic disturbance. We chose this day as a significant ionospheric storm day and Nov. 25, 2003 (DOY 329) was selected as an ionospheric quiet condition day.

ANALYSIS OF RESULTS AND DISCUSSIONS

For the processing scheme to generate the statistics, in general, there are two possible scenarios to estimate the VTEC in the network solution. The first one is a batch process and the second one is a baseline-by-baseline process. Both processes estimate the VTEC at each station along with the receiver and satellite IFBs. The difference between the two approaches is that the batch process uses all the collected 5 minutes (update interval) ionospheric measurements from all the stations in the network to estimate the VTEC and receiver IFBs for each station. Only one set of satellite IFBs is being estimated with the batch process. In the case of the baseline-by-baseline process, only data from two stations, the reference station (in our research, ALBH) and the monitoring station, are used. The reference station is needed to estimate the satellite and receiver IFBs which are relative to the receiver IFB of the reference station. The process is continuing until all the stations in the network are sequentially processed. In this case, sets of

satellite IFBs are available which depend on the number of baselines in the network.

The advantage of the batch process is that we can reduce the number of unknowns by estimating only one set of satellite IFBs in the network. It gives us an advantage to get more redundancies in terms of the estimation theory of minimizing the mean of the squared errors in the Kalman filter as long as the assumption that a satellite has a constant IFB for the whole network is valid for a day. There is also a further advantage by having more data in the batch process. As we have more measurements at a specific time (epoch), the variance is smaller and it causes a faster convergence in the estimation of satellite and receiver IFBs.

However, there is a disadvantage in the batch solution. The batch solution is stronger in terms of stability of the estimation but it is less sensitive to the local variation than the baseline-by-baseline process. The overall smoothing to the network in batch solution causes less sensitivity to local variations. Another disadvantage of the batch process is a long processing time.

However, as the quadratic approach needs more data as we are estimating three more spatial parameters than the bi-linear technique (see eqn. 2) and as it is far more sensitive to the density and distribution of ionospheric measurements, we used a batch process for processing an entire one-month's worth of data. The batch process also has some advantage to generate statistics as long as the statistics represent the overall (mean or smoothed) behavior.

We used a "super computer", the 164-processor Sun Microsystems V60 cluster at the University of New Brunswick to save processing time for the whole month's worth of data. To use the powerful capability of the super computer, a parallel processing technique has been implemented. A total of 10 processors are used together at the same time. The daily process used a priori information about the satellite and receiver IFBs from the previous run. This allowed us to use the parallel processing capability of the computer.

However for the sensitivity test, we used the baseline-by-baseline process and for the statistics we used the results from the batch process.

1. Not-monitored satellite effects

The explanation for "not-monitored satellite effects" on the regional ionospheric modeling can be made in two ways, in conceptual and mathematical terms.

For the conceptual view, in a global ionospheric model, it is possible to monitor all the satellites at any time using a

global scale network. This allows setting all the satellites and receivers' IFBs as unknowns within a single estimator. They remain in the Kalman filter during the entire estimation period and they are continuously estimated. However in the regional approach, this is no longer the case because only some of the satellites can be monitored by the ground network at any given time. As a result, only those satellites locally visible to the network at that time need to be updated using newly available measurements from the network.

The current UNB ionospheric model follows the global ionospheric model concept. An extension to the current UNB approach has been made for regional ionospheric modeling. The new concept works with a re-initialization process for the satellites which become visible to the network again sometime after they are first visible.

For the detailed mathematical description, in a general Kalman filter, even though there is a null column in the design matrix (H), which is caused by a not-monitored satellite at the specific epochs, it is still possible to invert the matrix, $(HP^T H^T + R)^{-1}$ to calculate the gain, as long as the measurement noise matrix, R, is positive definite and the matrix, $(HP^T H^T)$, is positive definite.

$$K = P^- H^T (HP^- H^T + R)^{-1} \quad (\text{eqn. 3})$$

where

K is the gain matrix, P⁻ is the a priori covariance matrix, H is the design matrix, and R is the measurement error covariance.

However, covariance effects occur for the matrix multiplication between the a priori covariance matrix and the design matrix, P⁻H^T. If there is any satellite which was not-monitored but set into the state vector, the covariance is continuously updated in the matrix P for the entire estimation. Furthermore, there is an issue for the observability [Gelb, 1974]. The observability condition is counted on the transition (Φ) and design matrix (H), $(H^T : \Phi^T H^T : \dots : (\Phi^T)^{n-1} H^T)$ to determine if there is a solution (matrix invertible). As long as a not-monitored satellite from the regional network at a specific epoch is set to null for one column in the design matrix, the possibility of an observability issue is raised.

The following Figure 3 shows the differences which are caused by the not-monitored satellites even though the effect of the covariance is small.

We selected the station BSMK from the CORS network: BSC Base which is located in Bismarck, North Dakota to see a more detailed view of the effect of a not-monitored satellite. The measurements at BSMK station have a relatively low noise in the network on DOY 329. The overall trends are similar for estimated VTEC and for residual time series. However there are small fluctuations

around 6:00 and 18:00 UTC when we used only monitored satellites. The differences can be explained by the differences in geometry. However we can clearly see the improvement in terms of residuals in the histogram (second panel) and time series of residuals (third panel).

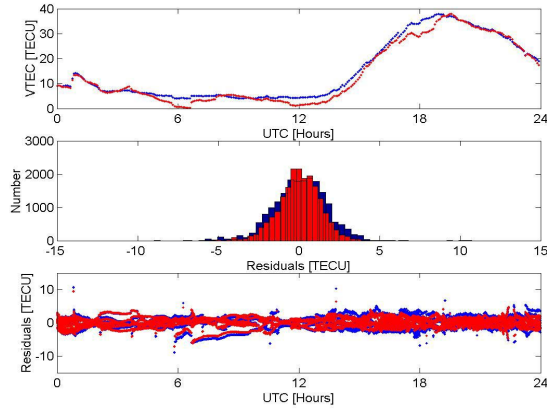


Figure 3. Comparison of the effects of not-monitored satellites, bi-linear model result on quiet day (DOY 329). The blue colors show the results when we set all the satellites in the estimator and the red colors show the results when we use and update only monitored satellites. The top panel shows the estimated VTEC at station BSMK. The second and third panels show the histogram and the time series of residuals, respectively.

The assumption for modeling the ionosphere was that the residual errors are following the zero mean Gaussian distribution. The distribution of residuals in Figure 3 is a bit improved when we used only the monitored satellites for the estimation (red color). The mean and standard deviation of residual errors was 0.073 and 1.634 TECU when we used all the satellites. It was 0.017 TECU and 1.301 TECU when we used only monitored satellites.

We generate the mean, the standard deviation (std.) and root mean square (rms) of residual errors by use of all the stations in the network for DOY 324 and DOY 329 to see what are the differences between them.

Unit: TECU	Quiet Day 329		Storm Day 324	
Bi-linear	Regional	Global	Regional	Global
mean	0.015	0.010	-0.014	-0.028
std.	1.442	1.704	4.488	4.931
rms	1.442	1.705	4.489	4.931
Quadratic	Regional	Global	Regional	Global
mean	0.012	0.040	0.012	0.046
std.	1.025	1.271	2.981	3.482
rms	1.025	1.271	2.982	3.482

Table 1. Statistics for residual errors for DOY 324 and 329. Where Regional represents the results when we used only monitored satellites and Global represents the results when we used all the satellites.

Table 1 shows there is more improvement in std. and rms than mean of residual errors in the regional approach especially when the ionosphere was disturbed. The overall differences for std. and rms on the quiet day were at about the 0.25 TECU level. However the difference of std. and rms on the storm day go up to the 0.5 TECU level. Table 1 also indicates what improvement we can expect when we use a quadratic model for storm conditions. The improvement of std. and rms of residuals was at about the 1.5 TECU level in both the regional and global approach.

The overall differences in VTEC and residuals, which are caused by not-monitored satellites, are small. However this is a valuable consideration in terms of stability to the system, when we use a higher order model.

2. Sensitivity Differences between Bi-linear and Quadratic Models

We made a sensitivity test between the bi-linear and quadratic models to characterize their different responses. If the variation of ionosphere does not follow the linear fashion, we should expect to see some improvement in terms of residual errors. As discussed in the description of data sets, we selected two sample days. DOY 329 as a quiet day and DOY 324 as a significant storm day were used to see the overall daily behavior of the ionosphere and to figure out if there is any improvement in terms of residual errors during ionospheric quiet and disturbed conditions. The TUNG (Tungsten) station near Oreana, Nevada, was selected to see the differences as a snap shot. The statistics of residuals for this station are closer than other stations to the overall mean of residual errors between different models for this day.

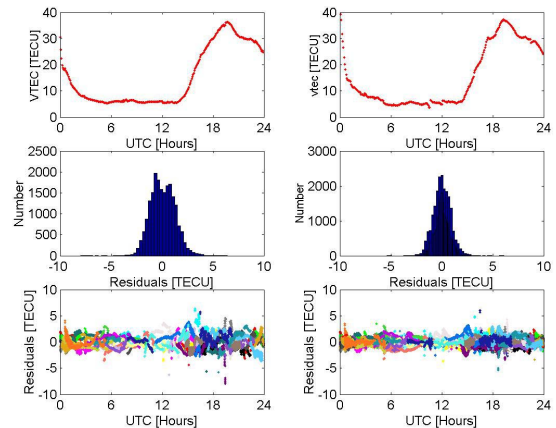


Figure 4. Sensitivity test between bi-linear (left panels) and quadratic (right panels) models at TUNG station on geomagnetic quiet day (DOY, 329). The first panel for each column shows the estimated vertical delays and the second panel shows the histogram of residuals and the third panel shows the time series of residuals.

In Figure 4, the VTECs in the quadratic model are a little more sensitive to the variations than the bi-linear results with generally the same trend and magnitude. The second order spatial variations in the quadratic model are allowed to depict more variations in estimated VTEC. The second panels show the distribution of residuals and the improvement in terms of residual errors by use of the 3 more spatial coefficients in the quadratic model. As we mentioned before, we expect that the residual errors would follow a zero mean Gaussian distribution. The residual errors in the quadratic approach are closer to the zero mean Gaussian assumptions. The mean of residuals in the bi-linear approach was 0.076 TECU and 0.038 TECU in the quadratic approach.

The third panels show the time series of residuals. We used a different color for each satellite to see individual improvement of satellites in terms of residuals. For the bi-linear case (left panel), PRN21 (purple) has not been very well explained (little spikes around 19:00 UTC) but those residuals are improved by the quadratic model. PRN26 was monitored two times, (around 4:00 to 8:00 and 19:00 to 23:00 UTC) by the network. The spikes occurred when the satellite comes in view again to the network. The quadratic approach is also able to better explain the measurement when the satellite is at low elevation angles. The third panels also show the different consistencies of the estimated residuals. The magnitudes of variations in residual errors are more consistent in the quadratic approach. The statistics reveal that there was 0.52 TECU improvements in terms of std. The std. for the bi-linear approach was 1.203 TECU and 0.698 TECU for the quadratic approach. As a summary, the quadratic approach seems stronger in being able to handle ionospheric variations based on the statistics.

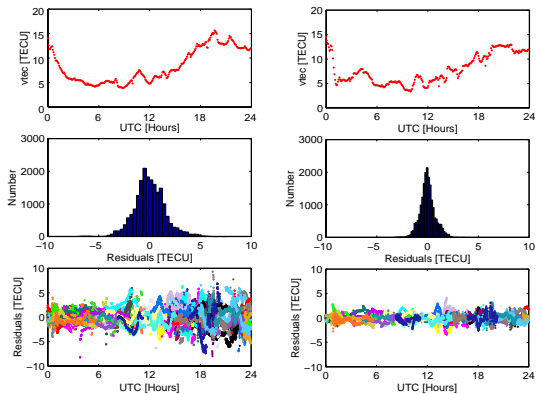


Figure 5. Sensitivity test between bi-linear (left panels) and quadratic (right panels) ionospheric models at TUNG station during significant geomagnetic storm conditions (DOY 324).

We further examined the quadratic model under significantly disturbed ionospheric conditions. So the Figure 5 shows the results with the same scenario as

Figure 4. In the first panels, there is a little difference in estimated VTEC in terms of trends and magnitudes between the bi-linear and quadratic models. In storm conditions, the residuals of the bi-linear model spread more widely compared with quiet-day residuals. And around 15:00 UTC, the residuals increased and continuously increase to the end of the day. The Dst index indicates that the significant geomagnetic disturbance started at 15:00 UTC. The Dst value was -198 nT at 15:00 and it went down quickly with a peak, -460 nT, at 21:00 UTC.

However, even during significant storm conditions, the quadratic approach seems to consistently well handle the ionospheric spatial and temporal variations. The third panel in Figure 5 shows the time variations of estimated ionospheric residuals. The mean of the residuals in the bi-linear model for this day was 0.021 TECU and 1.551 TECU for std. In quadratic approach, the daily mean is 0.021 TECU but the std. was 0.776 TECU. Even though there is statistically the same mean in the residual distributions, the standard deviation was improved by 0.774 TECU. However, the statistical improvement for this day shows the combined improvement between not significant storm condition (before 15:00 UTC) and significant storm condition (after 15:00 UTC). When the significant storm effects occurred (after 15:00 UTC), the improvement in rms of residual errors reached up to the 5 TECU level. It also shows the quadratic approach is stronger in terms of estimation when the ionosphere is more variable, as during storm conditions.

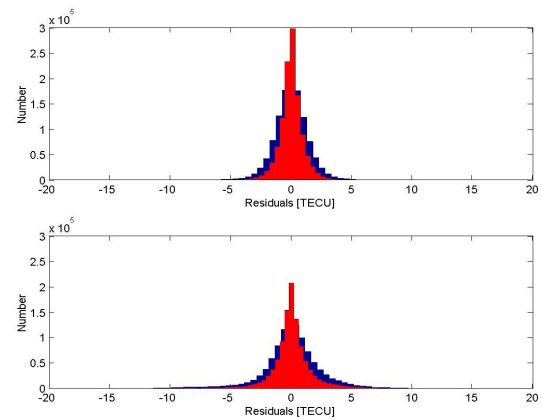


Figure 6. Comparison of residuals on the quiet day (DOY 329) and storm day (DOY 324). Top picture shows the distribution of residuals on DOY 329. The bottom picture shows the distribution of residuals on storm day (DOY 324). The red color represents quadratic results and blue color shows the bi-linear results.

In Figure 6, we compare all the residual errors between bi-linear and quadratic approaches from all the reference stations in the network. To see the overall differences in distribution of residuals for both the quiet and storm days, the X axis of both pictures have a range of ± 20 TECU

rather than the total range of residual errors. On the storm day, 10 residual errors were bigger than 100 TECU in the quadratic model and there were 169 residual errors which were bigger than 100 TECU in the bi-linear model. 99.997% of the residuals were at or below the 20 TECU (3.24 meter in L1 equivalent delays) level in quadratic model and 99.994% of residuals were at or below the 20 TECU level in the bi-linear model. In the case of quiet day, only 52 residuals in the bi-linear model and 13 residuals from the quadratic model were located outside of 20 TECU in the histogram. We used 20 TECU as a threshold to get rid of not very well modeled results from the statistics in the next section.

Without filtering the residuals to ± 20 TECU, the overall mean of the residuals for the quiet day was 0.016 TECU for bi-linear and 0.012 TECU for the quadratic model. The std. was 1.451 TECU for bi-linear and 1.028 TECU for quadratic results. On the storm day, the mean of residuals was 0.032 TECU and 0.022 TECU for bi-linear and quadratic models, respectively. And the std. was 6.050 TECU for bi-linear and 4.034 TECU for quadratic model. The total number of measurements was 1,151,804 on the quiet day and 1,150,183 on the storm day.

3. Spatial and Temporal Variation of the Residual Errors

To see the spatial variation of the residuals in latitude, we have divided the region of coverage into five bands, based on the location of stations in latitude. The latitude coverage of the monitoring stations extends from about 24.5 degrees to 50.9 degrees north. So we made a first band with the stations which are located above 45 degrees in latitude. From band 2 to 4, we used 5 degrees latitude spacing. And the stations which are located at less than 30 degrees in latitude were assigned to band 5.

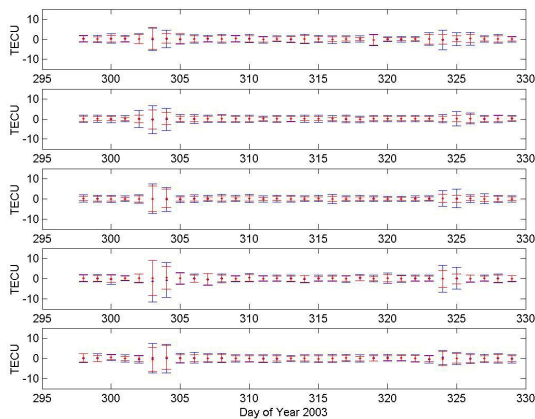


Figure 7. Comparison of the latitude variations of the daily mean and std. (error bars) of residuals between bi-linear and quadratic model. The blue color shows the results from the bi-linear model. The red color shows the results from the quadratic model.

The Figures 7 and 8 show the daily mean, std. and rms of residual errors in each band. First of all, the overall trend in daily mean residual errors is consistent between the bi-linear and quadratic approaches. The overall variation (maximum-minimum) of the mean of residual errors was 2.277 TECU (overall mean: 0.073 TECU) in bi-linear results and it was 1.060 TECU (overall mean: 0.082 TECU) for quadratic results. When the significant geomagnetic storms occurred, on DOY 302, 303, 304, 324 and 325, the std. of residuals dramatically increased and reached up to a maximum 10.160 TECU in the bi-linear and 8.596 TECU in the quadratic model. We further investigated the variation in the rms of residual errors.

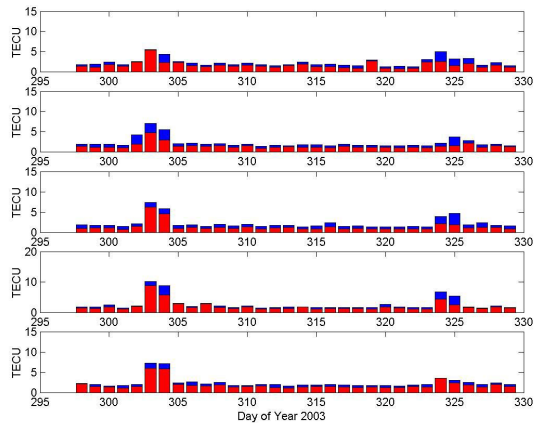


Figure 8. The latitude variation for the daily rms of residual errors. The blue color shows the results from bi-linear model. The red color shows the results from quadratic model.

Significant improvements in rms of residual errors occurred during the geomagnetic storm condition days. The improvement in rms of residuals was a maximum 1.515 TECU for quiet days and 3.134 TECU for storm condition days (see more detail, Table 2). However for DOY 307 in band 4, the residuals of bi-linear results were better to a maximum of 0.183 TECU than quadratic model results. After removing some un-modeled ionospheric residuals from the statistics, we could see sometimes the rms of residuals are better in the bi-linear model even though the magnitude of differences are less than 0.2 TECU. Perhaps the un-modeled ionosphere in the bi-linear model is much larger than that from the quadratic approach.

In Figure 8, the better improvements, compared with other bands on quiet days, are seen in band 3 which is located in the middle of the coverage area. It might be that the improvements are related to the density and distribution of measurements.

To see the spatial variation of the residuals in longitude, we divided the region into five bands, based on the longitude of the monitoring stations. The longitude coverage by the stations extended from about 63.6 degrees to 124.4 degrees west. The stations located to the west of longitude -110 degrees belong to the first band. From band 2 to 4, we used 10 degrees longitude spacing from west to east. And for the last band 5, we selected the stations which are located to the east of longitude -80 degrees. The following Figures 9 and 10 show the daily mean, std. and rms of residual errors in each section.

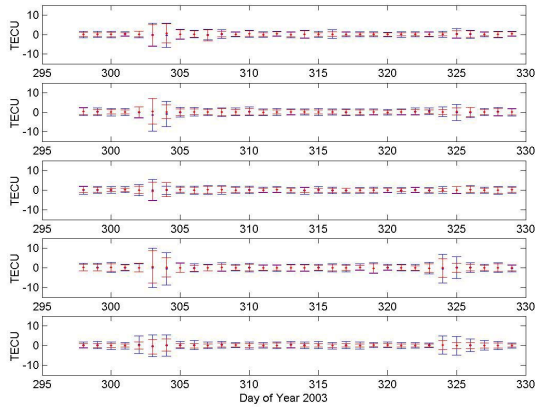


Figure 9. Comparison of the longitude variations of the daily mean and std. (error bars) of residuals between bi-linear and quadratic model. The blue color shows the results from the bi-linear model. The red color shows the results from the quadratic model.

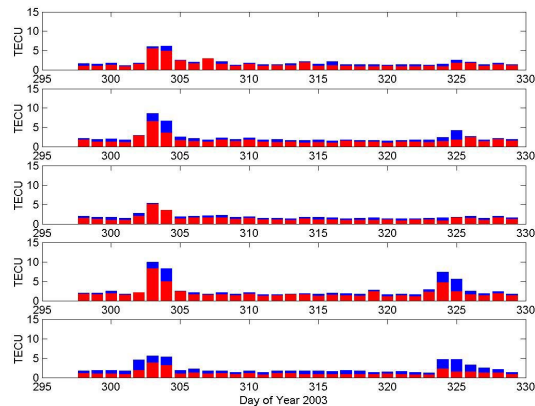


Figure 10. The longitude variation for the daily rms of residual errors. The blue color shows the results from bi-linear model. The red color shows the results from quadratic model.

In Figure 9, the overall variation in the mean of residual errors was 1.836 TECU (overall mean: -0.181 TECU) for bi-linear and for the quadratic results it was 1.080 TECU (overall mean: -0.122 TECU). The variation of std. for bi-linear was 8.84 TECU (maximum 9.918 TECU and minimum 1.034 TECU) and it was 7.516 TECU (max: 8.201 and min: 0.685) in the quadratic approach. In terms

of variation in the mean of the residuals, there is about a 0.7 TECU difference between the bi-linear and quadratic approaches.

In Figures 8 and 10, we can clearly see the rms of residuals increased when the geomagnetic storm occurred in both bi-linear and quadratic approaches. And the improvements of the rms by the quadratic model are also generally increased when the magnitudes of residual errors are increased. By comparing Figure 8 and 10 on DOY 324, we can see the more significant improvements occurred on the eastern side of the region at high latitudes. The daily UNB WAAS map [UNB Web, 2004] shows there were very fast fluctuations in the north eastern part of the U.S. However the ionosphere over the lower latitude eastern part of the U.S. for this day was characterized by not varying quickly but the magnitude of vertical delays were very big with slow change.

The better improvement in following fast variations might be explained by the dynamic model uncertainty, which we used for modeling the ionosphere on storm days. We allowed the model to follow a high 1 TECU per 2 minute change in the total electron content for dynamic ionospheric model uncertainty. In this case, the filter is more sensitive to the variation of measurements rather than previously estimated values.

In Figure 10, we can also see the better improvement of rms of residuals on quiet days occurred in band 5. There are more monitoring stations (denser distribution) located in band 5 (see Figure 1). It seems the density and distribution of measurements is the important factor for improving the residual rms by the quadratic model.

The following Table 2 shows the summarized statistics for residual rms. We subtracted the rms of residuals in the quadratic model from the rms of residuals in the bi-linear at each band to see the overall improvement in residuals by quadratic approach with different variations in latitude and longitude bands.

Unit: TECU	Latitude Bands		Longitude Bands	
	Quiet days	Storm days	Quiet days	Storm days
Mean	0.515	1.532	0.523	1.431
Max	1.305	3.134	1.494	3.212
Min	-0.183	-0.388	-0.102	-0.363

Table 2. Summarized statistics for the differences in residual rms between techniques for each band in both the latitude and longitude bands.

Table 2 shows that when the storms occurred, the overall residual rms increased about 1 TECU, compared with quiet days. The maximum improvements by use of quadratic model are about 3 TECU. The negative minimum values shows that sometimes the bi-linear

model was better in terms of residual errors. We need to further investigate, when and under what conditions, the bi-linear model explains the ionosphere better.

4. Comparison with WAAS Results

We found there are about 3 TECU differences in rms of residuals between the quadratic and bi-linear approaches when the ionosphere was disturbed. For validation purposes, we compared our estimated ionospheric vertical delays at each station with interpolated WAAS VTEC by use of the surrounding 4 grid points. We used 0.162m for 1 TECU to convert the units from TECU to meters of L1 delays as used by WAAS. The purpose of this validation is to investigate if the modeled ionosphere is reasonably well estimated, or if there is anything unphysical or abnormal in our models.

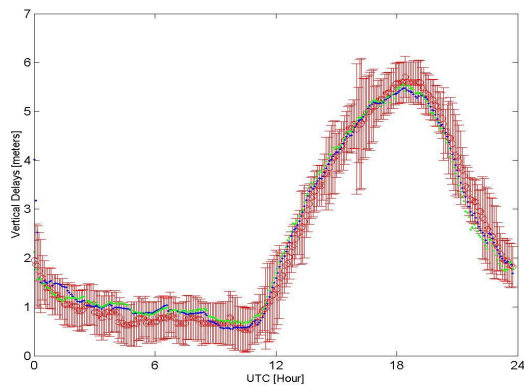


Figure 11. Comparison of vertical ionospheric delays (DOY 329, quiet day) in meters at the station PNB1. The blue dots represent the vertical ionospheric delays from our bi-linear model and the green dots show the estimated vertical ionospheric delays from the quadratic model. The red dots with error bars (one sigma) show the interpolated WAAS ionospheric vertical delays.

The UNB daily WAAS map [UNB Web, 2004] shows there were significant fluctuations in terms of vertical ionospheric delays when the geomagnetic field was disturbed on DOY 324 in the eastern U.S. The PNB1, Penobscot1, Penobscot, Maine, station was selected for the comparison of our estimated vertical ionospheric delays from both bi-linear and quadratic results with WAAS.

We interpolated the four WAAS ionospheric grid vertical delay values surrounding station PNB1 to vertical ionospheric delays at the station. For the statistics, we assume the WAAS vertical ionospheric delays as truth. The estimated vertical ionospheric delays from both the bi-linear and quadratic models were subtracted from the vertical ionospheric delays from WAAS.

For the ionospheric quiet condition day, the estimated vertical ionospheric delays from both bi-linear and

quadratic models at PNB1 have good agreement with WAAS. The uncertainty (one sigma) for WAAS (as given by the broadcast GIVE values) on the quiet day (DOY 329) was 1.333 meters in maximum, 0.409 meters for minimum and overall mean uncertainty was 0.501 meters.

Unit:	Quiet day		Storm day	
Meters	Bi-Linear	Quadratic	Bi-Linear	Quadratic
Mean diff	-0.045	-0.051	-0.103	-0.244
Mean std.	0.236	0.233	1.263	1.174
Mean rms	0.058	0.056	1.601	1.142

Table 3. Statistics for differences in vertical ionospheric delays from both bi-linear and quadratic models with WAAS at the station PNB1. Quiet day was Nov. 29 (DOY 329) and storm day was Nov. 24 (DOY 324), 2003.

We can see that both quadratic and bi-linear results are very close to those of WAAS and none of the estimated vertical ionospheric delays are outside the uncertainty bound of WAAS at the one sigma level. There are only 2 to 3 mm differences in terms of std. and rms. However in the case of mean differences, the results from the bi-linear model are a bit closer to those of WAAS. This can more clearly be seen on the storm condition day. There are 14cm mean differences between bi-linear and quadratic results. WAAS uses a first order (linear) planar fit ionospheric grid model. The mean differences might be explained by different orders of ionospheric model. However the statistics show the differences in std. and rms of the differences between UNB models and WAAS are increased during significant geomagnetic storm conditions.

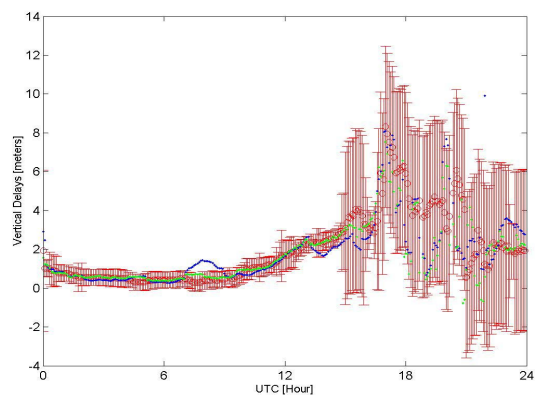


Figure 12. Comparison of vertical ionospheric delays (DOY 324, disturbed geomagnetic conditions day) in the units of meters at the station PNB1. The blue dots represent the vertical ionospheric delays from bi-linear model and the green dots show the estimated vertical ionospheric delays from quadratic model. The red dots with error bars (one sigma) show the interpolated WAAS ionospheric vertical delays.

Figure 12 shows the differences in the vertical ionospheric delays between UNB models and WAAS on a significant geomagnetic storm day. The uncertainty for WAAS dramatically increased when the geomagnetic disturbance started, about 15:00 UTC. The maximum uncertainty for WAAS reached up to 4.158 meters (0.416m for minimum, 1.262m in mean of day) at the one sigma level. However the fluctuation of the WAAS vertical ionospheric delays (more consistent even on significant geomagnetically disturbed days) are smaller than the UNB results. The fluctuations caused meter level differences in std. and rms.

The differences might also be explained by the fact that we allowed the model to follow a high 1 TECU per 2 minute change in the total electron content for dynamic ionospheric model uncertainty as we discussed before.

Our estimated vertical delays come from batch solutions for both the bi-linear and quadratic models. However there are different trends in vertical ionospheric delays between bi-linear and quadratic results, from 7 to 10 hours UTC as shown in Figure 12. We need further analysis for these differences.

To generate the overall statistics, which compare the estimated vertical delays by use of UNB models with WAAS, we selected nine monitoring stations from the network. The PLS1 (Polson1 in Polson, Montana), CASA (Mammoth Lakes Laser Station in Mammoth Lakes, California) and PLO3 (Point Loma 3 in San Diego, California) were selected to represent the western U.S. ionospheric delay behavior. BSMK (BSC Base in Bismarck, North Dakota), HVLK (Haviland in Haviland, Kansas) and ANG1 (Angleton1 in Angleton, Texas) have been selected to represent the ionospheric behavior in the middle of U.S. And finally we selected the stations PNB1 (Penobscot1 in Penobscot, Maine), NBR2 (New Bern2 in New Bern, North Carolina) and AOML (Atlantic Oceanographic & Met Lab in Miami, Florida) to represent the eastern part of the U.S.

Unit: Meters	Quiet Day, 329		Storm Day, 324	
	Linear	Quadratic	Linear	Quadratic
Mean	0.038	-0.028	0.349	0.325
std.	0.426	0.424	1.670	1.660
rms	0.407	0.395	1.908	1.680

Table 4. Statistics for differences of vertical ionospheric delays between UNB models and WAAS at nine selected stations.

In Table 4, the statistics show the quadratic and bi-linear models have good agreement when the ionosphere is quiet. However in storm conditions, the rms was a bit closer to WAAS by about 23cm with the quadratic model. However overall peak-to-peak variations of estimated

VTECs in both UNB quadratic and bi-linear models, were within the uncertainties of WAAS.

CONCLUSIONS AND FUTURE RESEARCH

In this paper we have compared the performance of the UNB bi-linear and quadratic ionospheric models in the U.S. during both quiet and storm days with a data set spanning one month from October 25 to November 25, 2003. As the quadratic model is far more sensitive to the distribution of ionospheric measurements, we have carefully selected 48 reference stations, mainly from the CORS and IGS networks

To select the processing model for our one-month data set, we examined the effect of “not-monitored satellites” on the estimator. In a global ionospheric model, all the satellites are monitored continuously by a global scale network. However in a regional ionospheric model, only some of the satellites can be seen by the ground network at a given time. We quantified the differences between the global approach and regional approach by continuously estimating all the satellite biases for the global approach and updating only the monitored satellites at each epoch using newly available measurements from the network for the regional model. On a quiet day, the difference in rms of residuals was about 0.25 TECU and it was 0.5 TECU when the ionosphere was disturbed. The technique might be valuable for modeling the ionosphere with a regional network, especially when the ionosphere is disturbed. This is also a valuable consideration in terms of stability of the system, when we use a higher order model.

The expected advantage of the quadratic model was the possibility to reduce the residual errors by better explaining the ionospheric variations by the help of the added spatial second order terms. In the differences between the quadratic and linear approaches, the overall trend of daily means have very good agreements between the two models. We found the most improvement in the quadratic approach is in the improvement of rms of residuals. In quiet conditions, the improvement of daily rms of residuals is at about the 1 (maximum 1.5) TECU level or less. The maximum improvement in rms of residuals happens when the ionosphere is significantly disturbed. The level of improvement is at the 1 to 3 TECU level.

For validation purposes, we compared the estimated ionospheric vertical delays from both the bi-linear and quadratic models with those of WAAS. UNB results are much more sensitive to the variations in the ionosphere. WAAS vertical ionospheric delays are more consistent even under significant ionospheric storm conditions than those of the UNB approaches. It causes a difference in the mean rms of about 1.9 meters in the bi-linear model. The differences might also be explained by the dynamic

ionospheric model uncertainty. We allowed the model to follow a high 1 TECU per 2 minute change in the total electron content. It made the Kalman filter more sensitive to the variation of measurements rather than estimated values from previous epochs. With the quadratic model, there was a better agreement with WAAS at the level of 23cm. However, overall peak-to-peak variations of estimated VTECs from both UNB quadratic and bi-linear models are within the uncertainties (one sigma) of WAAS.

The statistics show that the advantage of the quadratic approach is in the stability of the estimator when the ionosphere is highly variable, as during storm conditions. Future research will include investigating the improvements of vertical TEC estimations in the equatorial region by use of the UNB quadratic approach. It also will be valuable to compare the UNB quadratic results with other independent data sets, like those from the TOPEX or JASON altimetry spacecraft.

Finally, we saw that the improvement in the residual errors by the quadratic approach is more sensitive to the density and distribution of ionospheric measurements.

Further examination of the correlation analysis between density or distribution of measurements and improvement of residual errors in the quadratic model may be helpful to know the risks of the model and to have more rigorous statistics for its performance. Also the uncertainty of the dynamic model and correlation time analysis for the Kalman filter for quiet days and storm days may provide valuable information to further improve the results.

ACKNOWLEDGMENTS

The work reported in this paper was supported by the Natural Sciences and Engineering Research Council of Canada. The authors would like to thank the UNB Faculty of Computer Science for allowing us to use their "super computer" (164-processor Sun Microsystems V60 cluster). We also thank the U.S. Continuously Operating Reference Stations (CORS) and Scripps Orbit and Permanent Array Center (SOPAC) and their station operators for providing the GPS data.

REFERENCES

- Coco, D.S., C. Coker, S.R. Dahlke and J.R. Clynych (1991). "Variability of GPS Satellite Differential Group Delay Biases." *IEEE Transactions on Aerospace and Electronic Systems*, Vol. 27, No. 6, November, pp. 931-938.
- El-Arini, M.B., R. Conker, T. Albertson, J.K. Reagan, J.A. Klobuchar and P. Doherty (1994). "Comparison of Real-time Ionospheric Algorithms for a GPS Wide-area Augmentation system (WAAS)." *Navigation: Journal of The Institute of Navigation*, Vol. 41, No. 4, Spring 1994, pp. 393-413.
- Gelb, A. (Ed.) (1974). "Applied Optimal Estimation." Massachusetts Institute of Technology Press, Cambridge, Massachusetts, U.S.A., 374 pp.
- Hansen, A.J. (2002). *Tomographic Estimation of the Ionosphere Using Terrestrial GPS Sensor*. Ph. D. dissertation, Department of Electrical Engineering, Stanford University, CA, U.S.A., March 2002, 200 pp.
- Juan, J.M., A. Rius, M. Hernandez-Pajares and J. Sanz (1997). "A Two-layer Model of the Ionosphere Using Global Positioning System Data." *Geophysical Research Letters*, Vol. 24, No. 4, February 15, pp. 393-396.
- Komjathy, A. and R.B. Langley (1996). "The Effect of Shell Height on High Precision Ionospheric Modelling Using GPS." *Proceedings of the 1996 IGS Workshop*, Silver Spring, MD, 19-21 March, pp. 193-203.
- Komjathy, A. (1997). *Global Ionospheric Total Electron Content Mapping Using the Global Positioning System*. Ph. D dissertation, Department of Geodesy and Geomatics Engineering Technical Report No. 188, University of New Brunswick, Fredericton, Canada, 248 pp.
- Komjathy, A., B.D. Wilson, T.F. Runge, B.M Boulat, A. J. Mannucci, L. Sparker and M.J. Reyes (2002). "A New Ionospheric Model for Wide Area Differential GPS: The Multiple Shell Approach." *Proceedings of the Institute of Navigation National Technical Meeting*, The Institute of Navigation, San Diego, CA, U.S.A., 28-30 January, pp. 460-466.
- Mannucci, A.J., B. Iijima, L. Sparks, X. Pi, B. Wilson and U. Lindqwister (1999). "Assessment of Global TEC Mapping Using a Three Dimensional Electron Density Model." *Journal of Atmospheric and Solar-Terrestrial Physics*, Vol. 61, pp. 1227-1236.
- Sardon, E. and N. Zarraoa (1997). "Estimation of Total Electron Content Using GPS Data: How Stable are the Differential Satellite and Receiver Instrumental Biases?" *Radio Science*, Vol. 32, No. 5, September-October 1997, pp. 1899-1910.
- Schaer, S. (1999). *Mapping and Predicting the Earth's Ionosphere Using the Global Positioning System*. Ph.D dissertation, Astronomical Institute, University of Berne, 205 pp.
- Skone, S. (1998). *Wide Area Ionospheric Grid Modelling in the Auroral Region*. Ph.D. dissertation, Department of Geomatics Engineering, UCGE Reports No. 20123, University of Calgary, Calgary, Alberta, Canada, 198 pp.
- UNB Web (2004): "UNB Wide Area Augmentation System Monitoring Station", [On-line] September 19, 2004.
<<http://gauss.gge.unb.ca/WAAS/UNB.WAAS.html>>
- Wielgosz, P., O. Grejner-Brzezinska, I. Kashani and Y. Yi (2003). "Instantaneous Regional Ionosphere Modeling." *Proceedings of ION GPS 2003*, Portland, OR, 9-12 September, pp. 1750-1757.